

- microscale: Strategies and biological applications. *Sensors Actuators B* **38–39**: 29–37.
- KÜHL, M., AND N. P. REVSBECH. 2001. Microsensors for the study of interfacial biogeochemical processes, p. 180–210. *In* B. Boudreau and B. B. Jørgensen [eds.], *The benthic boundary layer*. Oxford Univ. Press.
- LEGENDRE, P., AND L. LEGENDRE. 1998. *Developments in environmental ecology*, 20. Numerical ecology, 2nd English edition. Elsevier Science.
- MORAN, P. A. P. 1950. Notes on continuous stochastic phenomena. *Biometrika* **37**: 17–23.
- NILSSON, H. C., AND R. ROSENBERG. 2000. Succession in marine benthic habitats and fauna in response to oxygen deficiency: Analyzed by sediment profiling-imaging and grab samples. *Mar. Ecol. Prog. Ser.* **197**: 139–149.
- RASMUSSEN, H., AND B. B. JØRGENSEN. 1992. Microelectrode studies of seasonal oxygen uptake in a coastal sediment: Role of molecular diffusion. *Mar. Ecol. Prog. Ser.* **81**: 289–303.
- REIMERS, C., AND R. N. GLUD. 2000. In situ chemical sensor measurements at the sediment-water interface, p. 249–282. *In* M. Varney [ed.], *Chemical sensors in oceanography*. Gordon and Breach Science Publishers.
- RHOADS, D. C., AND J. D. GERMANO. 1982. Characterization of organism-sediment relations using sediment profile imaging: An efficient method of remote ecological monitoring of the seafloor (Remots™ systems). *Mar. Ecol. Prog. Ser.* **8**: 115–128.
- TENGBERG, A., AND OTHERS. 1995. Benthic chamber and profile landers in oceanography—a review of design, technical solutions and functioning. *Prog. Oceanogr.* **35**: 253–294.

Received: 2 April 2001

Amended: 23 August 2001

Accepted: 6 September 2001

*Limnol. Oceanogr.*, 46(8), 2001, 2080–2087  
© 2001, by the American Society of Limnology and Oceanography, Inc.

## Measurement of local bed shear stress in streams using a Preston-static tube

**Abstract**—Local bed shear stress ( $\tau_w$ ) is a fluid dynamic parameter of importance in determining the physical and biological characteristics of stream-bed environments. Unfortunately, it is often difficult to measure  $\tau_w$  under field conditions. Herein we describe the use of a Preston-static tube, which is essentially a surface-mounted Pitot-static tube, to measure  $\tau_w$  in mountain streams. Our results indicate that it is possible to measure local shear stress quickly, consistently, and inexpensively in the field. This technique also provides high spatial resolution, which should allow for detailed in situ studies of local shear stress at scales relevant to lotic organisms. Such information will be invaluable in studies of benthic organisms and hydraulically relevant phenomena in the near-bottom zone of lotic systems.

There can be little doubt that near-bottom hydraulics, and shear stress ( $\tau$ ) in particular, remains one of the most important parameters for the study of bedload transport (e.g., Wilcock 1996; Blizard and Wohl 1998) and benthic ecology (e.g., Davis 1986; Carling 1992) in lotic environments. For example, one need only consider the Shield's curve, which predicts the movement of benthic sediments (e.g., Buffington and Montgomery 1997; Blizard and Wohl 1998), or examine the zonation of stream organisms (e.g., Robertson et al. 1997), to appreciate the importance of  $\tau$ . This is because  $\tau$  is partly a measure of the tractive (or frictional) forces per unit area of the bottom that results from the interaction of fluid moving past the bottom (i.e., the no-slip condition). The law of the wall,  $u = (u_* / \kappa) \ln(z/z_0)$ , where  $u$  is the mean streamwise velocity,  $u_*$  is the friction velocity given by  $u_* = \sqrt{\tau/\rho}$ ,  $\kappa$  is the von Karman constant,  $z$  is the distance from the wall or boundary, and  $z_0$  is the roughness height, can be used to determine  $u_*$  and thus  $\tau$  (e.g., Nowell and Jumars 1984; White 1999). At the reach scale in lotic systems, the total shear stress,  $\tau_0$ , which includes the local bed

shear stress (or skin friction,  $\tau_w$ ) and the form (or pressure) drag of the various elements in the stream (e.g., bars, boulders, logs), can be determined from the depth-slope product,  $\tau_0 = \rho g h S_o$ , where  $g$  is the acceleration due to gravity,  $h$  is the average water depth in the reach, and  $S_o$  is the surface slope (see Buffington and Montgomery 1999; Manga and Kirchner 2000). It is the local shear stress,  $\tau_w$ , however, that is a more appropriate parameter to measure at finer spatial scales corresponding to individual bed elements or biota.  $\tau_w$  is the subject of this report.

Whereas  $\tau_w$  is an essential hydraulic parameter to determine, there are a limited number of techniques that can be used to infer or to measure it (e.g., force balance methods, velocity profile methods, and mass transfer methods; Table 1; Winter 1977; Hanratty and Campbell 1983; Haritonidis 1989; Fernholz et al. 1996; Dade et al. 2001). For practical application under field conditions, these techniques fall into several categories, the most commonly used one of which uses vertical profiles or single or multiple measurements of velocity to estimate  $\tau_w$  based on the law of the wall. Advances in instrumentation for the measurement of water velocity, including constant temperature anemometry (CTA), laser-Doppler (LDV), acoustic Doppler (ADV), and particle image velocimetry (PIV), have increased the spatial and temporal resolution at which velocity is measured, providing an opportunity to estimate  $\tau_w$  and to compute Reynolds stresses from velocity fluctuations (e.g., Bouckaert and Davis 1998). Unfortunately, these techniques have limitations pertaining to their use under field conditions (e.g., CTA, LDV, and PIV; Hart et al. 1996; but see Tominaga and Nezu 1992, and Bertuccioli et al. 1999) and near boundaries (ADV; Finelli et al. 1999; Hoover and Ackerman pers. obs.), which are required in order to compute  $\tau_w$ . Moreover, the relatively high instrumentation cost of CTA, LDV, and PIV, and the time and effort required in both categories, limits their application in most field conditions.

An alternative approach to the measurement of  $\tau_w$  in the field is provided by the FST (Fließwasserstammtisch) method, which uses the movement of standardized hemispheres of different density on a platform to determine an integrated bed  $\tau$  (Statzner and Muller 1989). Whereas the FST method improves the spatial resolution for measuring  $\tau$ , there are difficulties as to how the hemispheres are deployed, how the bottom plate affects the near-bottom flow, how bottom topography affects results, which empirical relationship is used to infer  $\tau_w$ , and what is being measured (Frutiger and Schib 1993; Dittrich and Schmedtje 1995). It is apparent that a direct and inexpensive technique for accurately measuring local shear stress is lacking.

**Preston-tube methods:** There is, however, another type of technique for the measurement of  $\tau_w$  in laboratory settings, which uses pressure differences in the boundary layer to measure  $\tau_w$ . One of these techniques is the Preston tube, which involves the use of a surface-mounted Pitot tube to measure the total pressure ( $p_{\text{Tot}}$ ) at the boundary and a separate static (or piezometric) pressure tap ( $p_s$ ) (e.g., Preston 1954; Taheri and Bragg 1992). From dimensional reasoning, Preston (1954) suggested that the pressure differences in the viscous sublayer could be normalized by the fluid density ( $\rho$ ) and the kinematic viscosity ( $\nu$ ), which along with the shear stress are the only independent variables. Measurements are presented as plots of the nondimensional shear stress

$$y^* = \log_{10} \left( \frac{\tau_w d^2}{4\rho\nu^2} \right) \quad (1)$$

versus the nondimensional pressure difference

$$x^* = \log_{10} \left( \frac{\Delta p d^2}{4\rho\nu^2} \right) \quad (2)$$

where  $d$  is tube diameter and  $\Delta p = p_{\text{Tot}} - p_s$ . The following empirical relationship determined by Preston (1954)

$$y^* = -1.396 + \frac{7}{8}x^* \quad (3)$$

has been confirmed by others (e.g., for  $4.0 < x^* < 6.5$  and  $2.0 < y^* < 4.2$ ; see review in Ackerman et al. 1994). To be effective, the Preston tube must be small enough to be within the wall layer, pressure differences must be large, and the static pressure must be constant and measured close to the dynamic pressure tap. Regardless, Nece and Smith (1970) used a large Preston tube (3.8-cm diameter) and a separate static pressure tube to measure shear stress in rivers and estuaries, but their design is impractical for most applications in streams where the wall layer is smaller than the diameter of their device. Ackerman et al. (1994) addressed the aforementioned concerns in their development of a Preston-static tube, which combined Preston and static tubes into a single measurement device constructed from regular and side-bored syringe needles, respectively. The critical features of their construction were related to (1) the ratio of inner to outer diameter of the Preston tube, which should be  $>0.6$  (Bertelrud 1977), and (2) the ratio of the distance from the

leading edge to the tap of the static syringe ( $l$ ) to the diameter of the dynamic tap (i.e.,  $l/d$ ), which should be approximately  $>2$  to be beyond the influence of the local pressure gradient generated by tip of the syringe (Bertelrud 1977). Fortunately, these design parameters were within the specifications of commercially available stainless steel syringe needles (e.g., Hamilton Company), and direct comparisons with Preston tubes revealed that Preston-static tubes provided accurate and consistent measures of wall shear stress in the laboratory (Ackerman et al. 1994). The purpose of the present paper is to determine whether Preston-static tubes can be used to measure local shear stress in streams.

**Methods and materials**—Herein, we report on the direct measurement of shear stress in mountain streams using a Preston-static tube ( $p_{\text{Tot}}$  tap inner diameter = 0.56 mm and  $p_s$  tap diameter = 0.50 mm). Our device was constructed from a 20G-point style 5, 90° beveled tip syringe and a 20G side-bored point style 3 tip syringe needles (Hamilton Company) using the specifications reported in Ackerman et al. (1994). In this case, the ratio of inner to outer diameter of the Preston tube was 0.61, the ratio  $l/d$  was 1.65, and the static pressure tap was located adjacent to the total pressure tap to enable the detection of differences in water depth associated with turbulent flow (Fig. 1A). The Preston-static tube was mounted on a vertical support attached to an xyz-positioning frame (rectangular base with vertical point gauge; not shown) that was used in laboratory and field settings. A ball and socket connector was incorporated directly below the vertical support to provide fine-scale positioning of the Preston-static tube on the substrate (Fig. 1B). Flow visualization via a 20-cm long syringe needle (e.g., dye streaklines) was used to position the device within the principal flow direction. A three-way valve was incorporated into the tubing to allow the Preston-static tube to be purged of air bubbles, or debris in the case of high sediment loads. The pressure tubes lead to the differential pressure transducer (Model DP45–16, Validyne Engineering) where data were displayed.

**Results**—Calibration in a laboratory flow chamber: The Preston-static tube was calibrated in a laboratory flow chamber (20 cm  $\times$  20 cm  $\times$  200 cm, 10-cm water depth, with a smooth Plexiglas bottom) at different ambient velocities and angles of attack with respect to the total pressure tap. Fifteen observations recorded from the digital display of the pressure transducer over a period of 30 s were used to determine the mean and standard deviation of the measurements presented below. The first set of calibrations, which was conducted at middepth in the chamber at 130 cm downstream, compared velocity measurements obtained by the Preston-static tube with those obtained by an impeller velocimeter (Model 2100, Swoffer Instruments), and a Pitot-static tube (stagnation pressure [ $p_{\text{Tot}}$ ] tap inner diameter = 1.13 mm, static pressure [ $p_s$ ] tap diameter = 0.72 mm; Airflow Developments). The results were consistent in both cases ( $r^2 = 0.995$ ,  $r^2 = 0.994$ , respectively), although the Preston-static tube measured slightly higher velocities than the impeller velocimeter (Fig. 2). This is likely due to the larger volume of fluid sampled by the 5.02-cm diameter impeller in the 10-

Table 1. Techniques for measuring wall shear stress ( $\tau_w$ ). The measurement principle and the location of the device with respect to the bottom is indicated along with limitations and/or requirements for using the technique. The applicability of the technique to the field is also provided (Y = applicable, N = not applicable, ? = unknown/potentially applicable).

Measurement technique	Principal location	Limitations and/or requirements of technique	Field use	Reference
<b>I Direct techniques (i.e., not based on assumptions of the flow conditions)</b>				
<b>(A) Force balance techniques (based on the measurement of the force exerted on the boundary to estimate <math>\tau_w</math>)</b>				
(1) Floating-element balance (various types including micromachined floating elements)	Beneath/on (micromachined)	Difficulties with gaps and alignment of floating element; tradeoff between size and sensitivity of element; for use in flows with zero pressure gradients	N/?	Winter (1977); Hanratty and Campbell (1983); Haritonidis (1989); Fernholz et al. (1996)
<b>(B) Surface coating techniques (based on the measurement of the changes in the surface properties of the material to estimate <math>\tau_w</math>)</b>				
(1) Oil film interferometry	on	Requires visualization for data acquisition; no calibration needed; surface may be fouled	?	Fernholz et al. (1996)
(2) Liquid crystal and pressure-sensitive films/paints	on	Requires visualization for data acquisition; no calibration needed; surface may be fouled	?	Buttsworth et al. (2000)
<b>II Indirect techniques (i.e., based on assumptions of the flow conditions)</b>				
<b>(C) Momentum balance techniques (based on relating the momentum change in the flow to the force exerted by the wetted perimeter to estimate <math>\tau_w</math>)</b>				
(1) Pressure gradient in channels	—	Difficult to apply when the wetted area is not constant	Y/?	Haritonidis (1989)
(2) Momentum thickness	—	Difficult to apply to complex geometries	Y/?	Haritonidis (1989)
<b>(D) Wall similarity techniques (based on velocity or pressure measurements above and/or near the wall to estimate <math>\tau_w</math>)</b>				
<b>(1) Velocity profile techniques (i.e., based on the law of the wall)</b>				
(i) Depth-slope product	above	Provides a measure of $\tau_0$	Y	Chow (1959)
(ii) Near-bed velocity measurement or regression of the velocity profile	above	Technique is sensitive to the shape of the velocity gradient; $\geq 5$ observations are required in the logarithmic layer	Y	Nowell and Jumars (1984); Wilcock (1996); present study
(iii) Near-bed Reynolds stresses, and energy-dissipation techniques	above	High spatial and/or temporal resolution are required in the viscous sublayer and the logarithmic layer, respectively	Y/?	Dade et al. (2001)
<b>(2) Obstacle flow techniques (i.e., based on flow near the wall)</b>				
(i) Preston-tube techniques	on	Probe must be oriented correctly; limited use in highly accelerating flows, detached boundary layers, or where logarithmic law of wall is absent; relatively high $p_{\text{Tot}}$ needed for detection by manometer	Y	Preston (1954); Ackerman et al. (1994); Fernholz et al. (1996); present study
(ii) Surface obstacle techniques (Stanton-tube, subsurface fence, gate, block, step)	beneath	Does not depend on the logarithmic velocity profile; probes can be fouled	N	Haritonidis (1989); Fernholz et al. (1996)
(iii) FST hemispheres	on	Provides an integrated $\tau$ , boundary conditions are affected by the deployment platform	Y	Statzner and Muller (1989); Frutiger and Schib (1993); Dittrich and Schmedtje (1995)

Table 1. Continued.

Measurement technique	Principal location	Limitations and/or requirements of technique	Field use	Reference
(3) Mass/heat transfer techniques (i.e., relates mass/heat transfer to $\tau_w$ through calibration)				
(i) Heat transfer techniques (hot wire, pulsed wire, hot film)	on	Requires frequent calibration; sensitive to fouling of sensor; some types can be used where flow reversals occur	?	Hanratty and Campbell (1983); Gust (1988); Fernholz et al. (1996)
(ii) Dissolution and liquid transfer techniques	on	Dissolution rate affected by turbulent fluctuations; subject to fouling; material may affect surface conditions	?	Porter et al. (2000)
(iii) Polarographic (electrochemical) techniques	on/beneath	Difficulties associated with the choice of electrochemical system and interactions with the fluid	?	Haratty (1991)

cm depth used within the flow channel. This calibration with the Pitot-static tube indicates that the Preston-static tube also functions well as a Pitot-static tube when used away from the boundary.

The second set of calibrations was undertaken to determine whether the shear stress measured by the Preston-static tube was consistent with the regression method based on the law of the wall (e.g., Nowell and Jumars 1984), recognizing that Ackerman et al. (1994) demonstrated the consistency of the Preston-static tube with other methods (e.g., Preston tubes, drag in pipes). A velocity profile obtained using the Preston-static tube is presented in Fig. 3A. The shear stress was determined from  $u_*$  (i.e.,  $\tau = \rho u_*^2$ ) obtained from the product of  $\kappa$  and the slope of the plot of  $u$  versus  $\ln(z)$ , using the eight points nearest the boundary, which were found by inspection to be within the logarithmic region of the velocity profile. In this case the linear regression was significant and

meaningful ( $r^2 = 0.995$ ;  $P < 0.001$ ) and the equation was  $u = (0.063 \pm 0.002) \ln(z) + 0.73 \pm 0.01$ . The results obtained by this regression method ( $\tau_w = 0.612 \pm 0.001$  Pa, based on the mean  $\pm$  standard error of the regression coefficient) were greater than the  $\tau_w$  measured using the Preston-static tube deployed directly on the bottom ( $\tau_w = 0.439$  Pa), and the  $\tau_w$  obtained from the 1/7 power law approximation, which is determined from

$$\tau_w \approx \frac{0.0135 \mu^{1/7} \rho^{6/7} U^{13/7}}{x^{1/7}} \quad (4)$$

where  $\mu$  is the dynamic viscosity,  $U$  is the average velocity, and  $x$  is the downstream distance (see eq. 7.44 in White 1999) ( $\tau_w = 0.410$  Pa; see Table 2). The consistency of the  $\tau_w$  measured by the Preston-static tube and that determined by the 1/7 power law approximation is satisfying given that the latter was shown by Prandtl to be a reasonably good approximation to the velocity gradient obtained for turbulent flow over a flat plate (i.e., the bottom of the flow channel used here; White 1999). Similar results were obtained for the other velocity gradients presented in Fig. 3B (Table 2). That the Preston-static tube method provided results that were different from the regression method is not unexpected given the uncertainty in the regression method, especially with respect to the shape of the velocity profile (see Wilcock 1996). Specifically, the average difference between  $\tau_w$  obtained from the Preston-static tube and the regression analysis was 39% versus 8% for the difference between the Preston-static tube and the 1/7 power law approximation (i.e., Eq. 4). The Preston-static tube technique thus appears to provide reasonably consistent estimates of local wall shear stress.

The final calibration of the device involved the determination of the effect of yaw, or angle of attack, on the shear stress measurements. The Preston-static tube was deployed on the bottom of the flow chamber and was rotated between  $\pm 60^\circ$  in  $10^\circ$  increments from the approaching flow direction defined as  $0^\circ$  (Fig 4A). Results indicate that angle of attack has an important effect on the shear stress, and that this

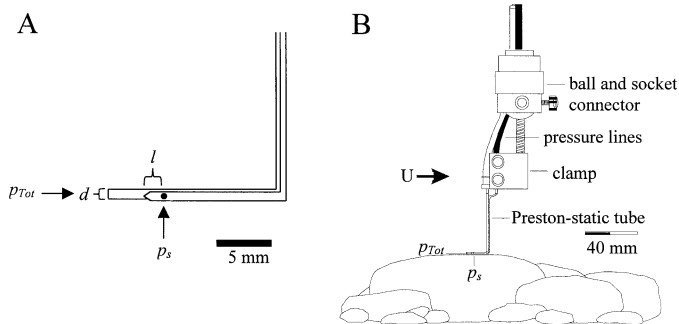


Fig. 1. (A) The Preston-static tube uses the difference between the total pressure ( $p_{Tot}$ ) and static pressure ( $p_s$ ) to measure local shear stress. The inner diameter of the  $p_{Tot}$  tap ( $d$ ) along with the distance from the leading edge to the tap of the static syringe ( $l$ ) are indicated. The diameter of the 20G syringe needles has been exaggerated for clarity. See text and Ackerman et al. (1994) for additional details. (B) Deployment device used to position the Preston-static tube in the laboratory and in mountain streams, which is mounted to a vertical support and attached to an  $xyz$ -positioning device (not shown).

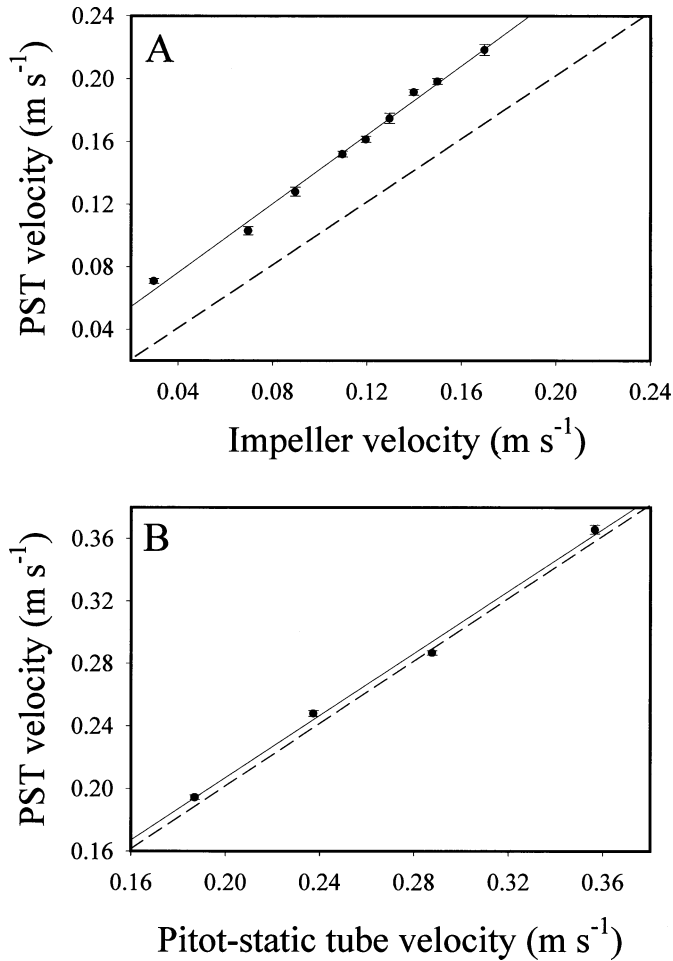


Fig. 2. Comparison of velocity measurements obtained by the Preston-static tube (PST) with those obtained by (A) an impeller velocimeter and (B) a Pitot-static tube at midchannel depth in the laboratory flow chamber. The solid line is a linear regression, the dotted line is a line of unity (i.e.,  $y = x$ ), and the error bars represent the standard deviation.

effect increases with ambient velocity (Fig. 4B). The results show a somewhat dome-shaped curve with the apex at  $0^\circ$ . The asymmetry between the left and right side of the dome is due to the placement of the static tap in the lee of the dynamic tap at negative angles of attack. The results obtained within  $\pm 20^\circ$  will likely be most consistent with  $\tau_w$  measured in the direction of flow (i.e.,  $0^\circ$ ), which indicates the importance of the proper orientation of the Preston-static tube in the field.

**Field deployment:** The Preston-static tube was deployed in four streams within the Torpy River watershed of the McGregor Mountains approximately 90 km east of Prince George, British Columbia. Velocity gradient and local shear stress measurements were obtained in a stream at km 25.8 along the lower Torpy River logging road. This reach had a relatively smooth gravel bottom and the flow was subcritical as indicated by the channel Froude number ( $Fr = U/\sqrt{gD}$  = 0.41, where  $D$  is the water depth; Fig. 5). The Preston-

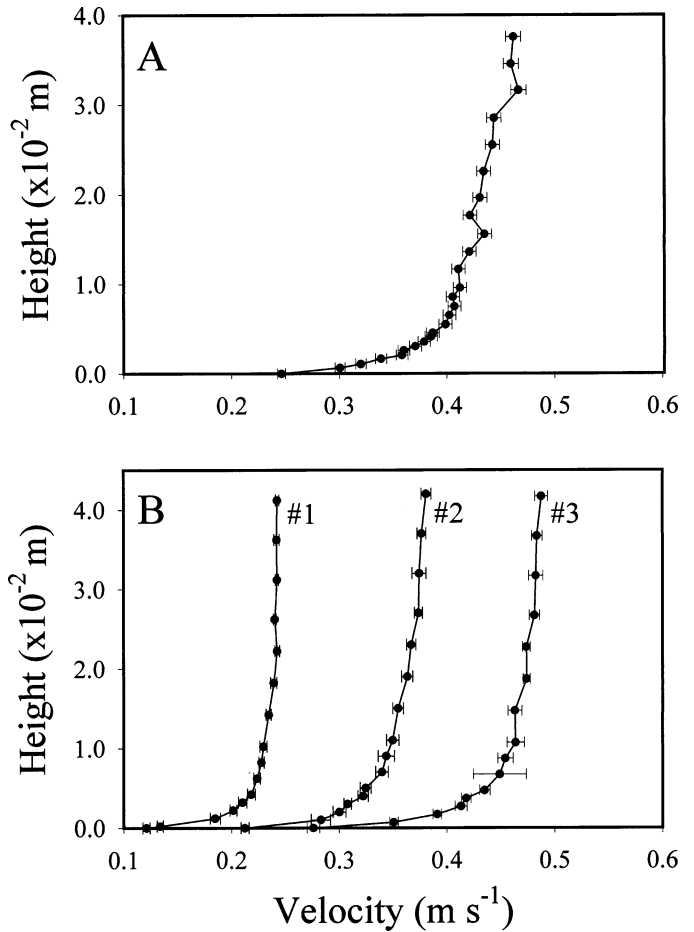


Fig. 3. (A) A velocity profile obtained within the laboratory flow chamber using a Preston-static tube as a Pitot-static tube (estimated measurement error of 1.5%). (B) Examples of other velocity profiles obtained in the same manner. Error bars represent the standard deviation. The shear stress determined for these profiles is presented in Table 2.

static tube was deployed parallel to the surface of a well-sorted reasonably flat reach (i.e., without large substrate elements present) containing smooth gravels (0.5–5 cm in diameter), and oriented into the flow as indicated by flow visualization. The shear stress measured by the Preston-static tube and the regression methods were reasonably consistent, as in the case of the laboratory ( $\tau_w = 0.217 \pm 0.007$  Pa,  $\tau_w = 0.277 \pm 0.002$  Pa, respectively).

Direct measurements of local shear stress were made in three streams located at km 9, 12, and 22 of the lower Torpy River logging road. The streams were selected for similar average water depth ( $0.06 \pm 0.01$ ,  $0.11 \pm 0.01$ , and  $0.14 \pm 0.02$  m, respectively), width (1.1, 2.9, and 3.0 m, respectively), slope (3.2%, 1.2%, and 2.2%, respectively), discharge ( $0.030$ ,  $0.055$ , and  $0.15$  m<sup>3</sup> s<sup>-1</sup>, respectively), and average velocity ( $0.48 \pm 0.04$ ,  $0.18 \pm 0.02$ , and  $0.3 \pm 0.1$  m s<sup>-1</sup>, respectively). The beds of these shallow streams included boulders (i.e., elements >30 cm), cobble (7.5–30 cm), and gravel (0.4–7.5 cm) in the following relative proportions (i.e., boulder:cobble:gravel): 0:5:90; 0:65:30;

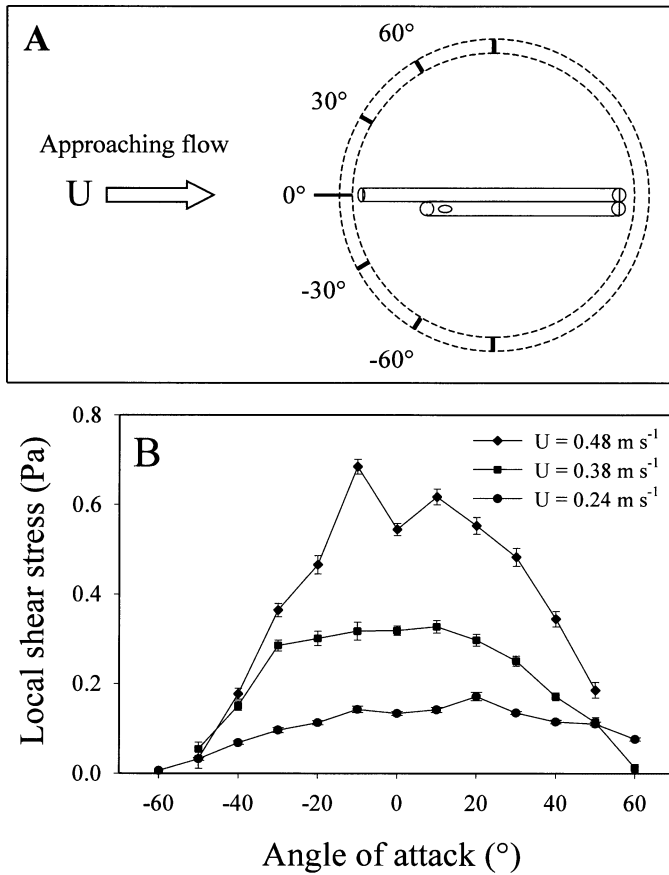


Fig. 4. (A) Schematic drawing of the arrangement used to determine the effects of angle of attack (i.e., yaw) on the local shear stress measured with a Preston-static tube. (B) Plots of the shear stress measured at different angles of attack for three ambient flow chamber velocities. Error bars represent the standard deviation.

and 30:20:35, in the respective streams. Eight or nine measurement locations were chosen within each stream where substrates with relatively flat surfaces could be found. The depths at which the local shear stress measurements were made ranged from  $0.047$  to  $0.20$  m, with an average depth of  $0.12 \pm 0.02$ ,  $0.083 \pm 0.007$ , and  $0.105 \pm 0.009$  m, in the respective streams (Table 3). The average streamwise velocity measured at 60% water depth ranged from  $0.23$  to  $0.67$   $\text{m s}^{-1}$ , with an average velocity of  $0.42 \pm 0.05$ ,  $0.48 \pm 0.04$ , and  $0.53 \pm 0.05$   $\text{m s}^{-1}$ , respectively (Table 3). The conditions at the measurement location were consistent among streams given the Reynolds number ( $Re$ ) based on the water depth, and the  $Fr$  determined among streams (i.e., average  $Re \sim 4$  to  $5 \times 10^4$  and average  $Fr \sim 0.4$  to  $0.5$ ; Table 3). The local shear stress measured with the Preston-static tubes varied within and among streams, with a range of  $0.1$  to  $3.8$  Pa. The average local shear stress was  $0.8 \pm 0.2$ ,  $1.4 \pm 0.3$ , and  $2.0 \pm 0.4$  Pa in the three streams (Table 3). These  $\tau_w$  values were a fraction of the total shear stress,  $\tau_0$ , provided by the depth-slope product (Table 3), which is consistent with the partitioning of shear stress due to the high form drag contributed by large bed forms in these type

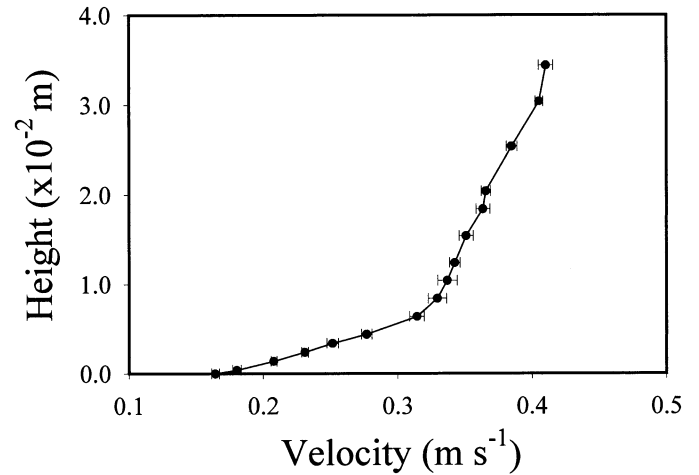


Fig. 5. A velocity profile measured over flat gravels (0.5 to 5 cm in length) using a Preston-static tube in the stream at km 25.8 of the lower Torpy River Road.

of shallow mountain streams (Hart et al. 1996; Buffington and Montgomery 1999; Manga and Kirchner 2000).

*Discussion*—The Preston-static tube is a relatively good instrument for the measurement of wall shear stress ( $\tau_w$ ) in the laboratory and field when compared to conventional approaches and theoretical predictions (*see above* and Tables 1 and 2). Moreover it can also be used as a Pitot-static tube with fine spatial resolution when used outside the wall layer (Figs. 2, 3, and 5). Care must be taken to orient the instrument into the approaching flow, although the results are reasonably consistent for yaws of  $\pm 20^\circ$  from the principal flow direction (Fig. 4). It should be noted, however, that while we successfully used the Preston-static tube to measure shear stress under mean velocities of  $20$   $\text{cm s}^{-1}$  and as a Pitot-static tube to measure velocities as low as  $5$   $\text{cm s}^{-1}$ , this instrument will be limited by the ability to measure pressure difference determined primarily by the dynamic pressure of the flow. We found that our configuration was somewhat limited in areas of turbulent recirculation or separation (e.g., on the downstream edges of substrates) where rapidly changing flow directions and water depths made it difficult to orient the device and to record fluctuations. The use of a fast response pressure transducer and a data logger would be

Table 2. Comparison of local shear stress ( $\tau_w$ ) obtained from the data presented in Fig. 3 using different techniques.

Velocity profile	Local shear stress $\tau_w$ measurement (Pa)		
	Preston-static tube	Law of the wall regression	1/7 Power law (Eq. 4)
Profile in Fig. 3A	$0.439 \pm 0.006$	$0.612 \pm 0.001$	0.410
Profile 1 in Fig. 3B	$0.127 \pm 0.006$	$0.269 \pm 0.002$	0.128
Profile 2 in Fig. 3B	$0.339 \pm 0.002$	$0.328 \pm 0.002$	0.299
Profile 3 in Fig. 3B	$0.536 \pm 0.008$	$0.559 \pm 0.001$	0.463

Table 3. Fluid dynamic conditions measured at the sampling locations in three streams along the lower Torpy River logging road. Data are reported as mean  $\pm$  SE with the range of values indicated in parentheses.

Stream location	Total shear stress, $\tau_0$ (Pa)	Parameters measured/determined at the site of Preston-static tube deployment				
		Depth (m)	Velocity (m s <sup>-1</sup> )	Re $\times 10^4$	Fr	Local shear stress, $\tau_w$ (Pa)
9 km ( $N = 8$ )	18.8	0.12 $\pm$ 0.02 (0.05–0.20)	0.42 $\pm$ 0.05 (0.23–0.67)	5 $\pm$ 1 (1.1–9.5)	0.40 $\pm$ 0.04 (0.29–0.61)	0.8 $\pm$ 0.2 (0.12–2.1)
12 km ( $N = 9$ )	12.9	0.083 $\pm$ 0.007 (0.05–0.105)	0.48 $\pm$ 0.04 (0.24–0.64)	4.0 $\pm$ 0.5 (1.5–5.5)	0.54 $\pm$ 0.05 (0.30–0.85)	1.4 $\pm$ 0.3 (0.10–3.2)
22 km ( $N = 8$ )	30.2	0.105 $\pm$ 0.009 (0.06–0.13)	0.53 $\pm$ 0.05 (0.33–0.75)	5.4 $\pm$ 0.5 (4.0–8.4)	0.55 $\pm$ 0.08 (0.29–0.98)	2.0 $\pm$ 0.4 (0.42–3.82)

useful in these situations. Regions with either high sediment loads and/or air entrainment in the flow will require frequent flushing of the pressure ports and may limit the applicability of the device. Regardless, the Preston-static tube will be most effective in regions with well-developed and unidirectional flow conditions and has provided subcentimeter-scale resolution for the measurement of  $\tau_w$  in the laboratory (i.e., 0.5-cm intervals in Ackerman et al. 1995).

It was possible to use the Preston-static tube in the field to measure local shear stress on a variety of substrates and under a range of local conditions (Table 3). On average the  $\tau_w$  measured were consistent with measurements made in the laboratory. For example, the average  $\tau_w$  measured in the stream at 9 km was within a factor of 1/3 of the  $\tau_w$  measured in the laboratory flume at comparable velocity (e.g., profile 3 in Table 2). Notwithstanding the important differences between a laboratory flow channel and a mountain stream, the consistency in measurement suggest that the Preston-static tube provides a reasonable measure of local shear stress in the field. This assertion is also supported by the data obtained in the stream at km 25.8 where the Preston-static tube method compared well with the regression method using the velocity profile in Fig. 5. Given the roughness of the stream bed and shallowness of these streams, it was not surprising that the local shear stress represented only a small proportion of the total shear stress predicted within a reach (Table 3) (Buffington and Montgomery 1999; Manga and Kirchner 2000). This indicates that the distribution and magnitude of  $\tau_w$  is more variable than suggested by other techniques (e.g., FST) and approximations of  $\tau$ . It is evident that additional research is needed to ascertain the effect of local influences (e.g., pressure gradients, substrate shape, and spacing) and the spatial distribution of local shear stress in lotic systems. The Preston-static tube technique should help to facilitate this need.

The results of this study indicate that it is possible to measure local bed shear stress accurately, quickly, and inexpensively under field conditions using a Preston-static tube. This technique provides high spatial resolution, which should allow detailed surface contouring of shear stress on substrates in situ. Such data will be useful in the characterization of microhabitats of benthic organisms and other hydraulically relevant phenomena in the near bottom of lotic systems.

Josef Daniel Ackerman<sup>1</sup> and Trent M. Hoover

Physical Ecology Laboratory,  
University of Northern British Columbia  
Prince George, British Columbia, Canada V2N 4Z9

### References

- ACKERMAN, J. D., C. M. COTTRELL, C. R. ETHIER, D. G. ALLEN, AND J. K. SPELT. 1995. A wall jet to measure the attachment strength of zebra mussels. *Can. J. Fish. Aquat. Sci.* **52**: 126–135.
- , L. WONG, C. R. ETHIER, D. G. ALLEN, AND J. K. SPELT. 1994. Preston-static tubes for the measurement of wall shear stress. *J. Fluids Eng.* **116**: 645–649.
- BERTELUD, A. 1977. Total head/static measurements of skin friction and surface pressure. *AIAA J.* **15**: 436–438.
- BERTUCCIOLI, L., G. I. ROTH, J. KATZ, AND T. R. OSBORN. 1999. A submersible particle image velocimetry system for turbulence measurements in the bottom boundary layer. *J. Atmos. Ocean. Technol.* **16**: 1635–1646.
- BLIZARD, C. R., AND E. E. WOHL. 1998. Relationships between hydraulic variables and bedload transport in a subalpine channel, Colorado Rocky Mountains, U.S.A. *Geomorphol.* **22**: 359–371.
- BOUCKAERT, F. W., AND J. DAVIS. 1998. Microflow regimes and the distribution of macroinvertebrates around stream boulders. *Freshw. Biol.* **40**: 77–86.
- BUFFINGTON, J. M., AND D. R. MONTGOMERY. 1997. A systematic analysis of eight decades of incipient motion studies, with special reference to gravel-bedded rivers. *Water Resour. Res.* **33**: 1993–2029.
- , AND ———. 1999. Effects of hydraulic roughness on surface textures of gravel-bed river. *Water Resour. Res.* **35**: 3507–3521.
- BUTTSWORTH, D. R., S. J. ELSTON, AND T. V. JONES. 2000. Skin

<sup>1</sup> Mailing address: Natural Resources and Environmental Studies, University of Northern British Columbia, 3333 University Way, Prince George, British Columbia, Canada V2N 4Z9 (ackerman@unbc.ca).

### Acknowledgments

The authors would like to thank Sheldon Lovell of the Department of Civil and Environmental Engineering at the University of Alberta for the loan of the pressure transducer. We are grateful to Greg Lawrence, Heidi Nepf, Mark Loewen, Margaret Palmer, and several anonymous reviewers for commenting on the manuscript. Support for this research was provided by the Natural Sciences and Engineering Research Council of Canada (NSERC) and Forest Renewal British Columbia (FRBC) to J.D.A.

- friction measurements on reflective surfaces using nematic liquid crystal. *Exp. Fluids* **28**: 64–73.
- CARLING, P. A. 1992. The nature of the fluid boundary layer and the selection of parameters for benthic ecology. *Freshw. Biol.* **28**: 273–284.
- CHOW, V. T. 1959. *Open-channel hydraulics*. McGraw-Hill.
- DADE, W. B., A. J. HOGG, AND B. P. BOUDREAU. 2001. Physics of flow above the sediment-water interface, p. 4–43. *In* B. P. Boudreau and B. B. Jørgensen [eds.], *The benthic boundary layer*. Oxford Univ. Press.
- DAVIS, J. A. 1986. Boundary layers, flow microenvironments and stream benthos, p. 293–312. *In* P. De Deckker and W. D. Williams [eds.], *Limnology in Australia*. Junk.
- DITTRICH, A., AND U. SCHMEDTJE. 1995. Indicating shear stress with FST-hemispheres—effects of stream-bottom topography and water depth. *Freshw. Biol.* **34**: 107–121.
- FERNHOLZ, H. H., G. JANKE, M. SCHÖBER, P. M. WAGNER, AND D. WARNACK. 1996. New developments and applications of skin-friction measuring techniques. *Meas. Sci. Technol.* **7**: 1396–1409.
- FINELLI, C. M., D. D. HART, AND D. M. FONSECA. 1999. Evaluating the performance of an acoustic Doppler velocimeter in near-bed flows. *Limnol. Oceanogr.* **44**: 1793–1801.
- FRUTIGER, A., AND J. L. SCHIB. 1993. Limitations of FST hemispheres in lotic benthos research. *Freshw. Biol.* **30**: 463–474.
- GUST, G. 1988. Skin friction probes for field applications. *J. Geophys. Res.* **93C**: 14121–14132.
- HANRATTY, T. J. 1991. Use of the polarographic method to measure wall shear stress. *J. Appl. Electrochem.* **21**: 1038–1046.
- , AND J. A. CAMPBELL. 1983. Measurement of wall shear stress, p. 559–615. *In* R. J. Goldstein [ed.], *Fluid mechanics measurements*. Hemisphere.
- HARITONIDIS, J. H. 1989. The measurement of wall shear stress, p. 229–261. *In* M. Gad-el-Hak [ed.], *Advances in fluid mechanics measurements*. Springer.
- HART, D. D., B. D. CLARK, AND A. JASENTULYANA. 1996. Fine-scale field measurements of benthic flow environments inhabited by stream invertebrates. *Limnol. Oceanogr.* **41**: 297–308.
- MANGA, M., AND J. W. KIRCHNER. 2000. Stress partitioning in streams by large woody debris. *Water Resour. Res.* **36**: 2373–2379.
- NECE, R. E., AND J. D. SMITH. 1970. Boundary layer stress in rivers and estuaries. *J. Waterw. Harb. Res.* **96**: 335–358.
- NOWELL, A. R. M., AND P. A. JUMARS. 1984. Flow environments of aquatic benthos. *Annu. Rev. Ecol. Syst.* **15**: 303–328.
- PORTER, E. T., L. P. SANFORD, AND S. E. SUTTLES. 2000. Gypsum dissolution is not a universal integrator of ‘water motion’. *Limnol. Oceanogr.* **45**: 145–158.
- PRESTON, J. H. 1954. The determination of turbulent skin friction by means of Pitot tubes. *J. R. Aeronaut. Soc.* **58**: 109–121.
- ROBERTSON, A. L., J. LANCASTER, L. R. BELYEA, AND A. G. HILDREW. 1997. Hydraulic habitat and the assemblage structure of stream benthic microcrustacea. *J. N. Am. Benthol. Soc.* **16**: 562–575.
- STATZNER, B., AND R. MULLER. 1989. Standard hemispheres as indicators of flow characteristics in lotic benthos research. *Freshw. Biol.* **21**: 445–459.
- TAHERI, M., AND G. M. BRAGG. 1992. A study of particle resuspension in a turbulent flow using a Preston tube. *Aerosol Sci. Tech.* **16**: 15–20.
- TOMINAGA, A., AND I. NEZU. 1992. Velocity profiles in steep open-channel flows. *J. Hydraul. Eng.* **118**: 73–90.
- WHITE, F. M. 1999. *Fluid Mechanics*. 4th ed. McGraw Hill.
- WILCOCK, P. R. 1996. Estimating local bed shear stress from velocity observations. *Water Resour. Res.* **32**: 3361–3366.
- WINTER, K. G. 1977. An outline of the techniques available for the measurement of skin friction in turbulent boundary layers. *Prog. Aerospace Sci.* **18**: 1–57.

Received: 23 October 2000  
Amended: 24 August 2001  
Accepted: 28 August 2001

## The optics of chromophoric dissolved organic matter (CDOM) in the Greenland Sea: An algorithm for differentiation between marine and terrestrially derived organic matter

**Abstract**—The optics of chromophoric dissolved organic matter (CDOM) in the Greenland Sea were investigated and compared to results from earlier studies in the Southeastern North Sea. Absorption at 375 nm ( $a_{375}$ ) in the Greenland Sea varied from 0.77  $\text{m}^{-1}$  to the detection limit of our instrument (0.05  $\text{m}^{-1}$ ), with the highest values found during summer. The spectral slope coefficient ( $S$ ) ranged from 8.2 to 26.4  $\mu\text{m}^{-1}$  with the highest values occurring during winter. Seasonal variations in the in situ production and degradation of CDOM were shown to be responsible for the trends seen. A negative correlation between  $S$  and  $a_{375}$  was evident in the Greenland Sea and differed noticeably from that found in coastal waters. The differing  $S$ - $a_{375}$  behavior of CDOM known to be of terrestrial origin allowed the development of an algorithm for the differentiation between marine and terrestrial organic matter. The behavior of marine CDOM was modeled by  $S = 7.4 + 1.1/a_{375}$ .

Chromophoric dissolved organic matter (CDOM) exists in all natural waters. Its source is the degradation of plant ma-

terial of both terrestrial and aquatic origin (Kirk 1994). In coastal waters it is present in large quantities due to runoff from rivers and it is responsible for a major part of the attenuation of photosynthetically available radiation (PAR). Although it exists at substantially lower concentrations in oceanic environments, it still plays a significant role for the attenuation of light in the water column. The absorption of light by CDOM is strongest in the UV region and approaches zero with increasing wavelength. The behavior can be modeled using this exponential equation,

$$a_{\lambda} = a_{\lambda_0} e^{S(\lambda_0 - \lambda)} \quad (1)$$

where  $a_{\lambda}$  and  $a_{\lambda_0}$  are the absorption coefficients at a certain wavelength and a reference wavelength, respectively, and  $S$  is the spectral slope coefficient that determines the shape of the absorption curve (Jerlov 1968; Lundgren 1976; Bricaud et al. 1981).

CDOM's light absorption properties can result in both a positive and a negative feedback on aquatic organisms. In